# APPROXIMATE COMPUTATIONAL FORMULAS FOR FAST CALCULATION
## OF HEAVY WATER THERMODYNAMIC PROPERTIES

## A.P. Firla

## Ontario Hydro, Toronto, Nuclear Studies and Safety Department

Abstract: For fast, repeated calculations of the heavy water
thermodynamic properties such as those occurring in CANDU PHWR safety
studies, linear interpolation algorithms to the $D_2O$ thermodynamic
tables are commonly used. Such an approach, while being direct and
relatively simple is not necessarily the most efficient. An alternative
approach using simple low order numerical functions to approximate the
$D_2O$ thermodynamic properties has been developed. These approximations
are presented and provide means for rapid calculation of the $D_2O$
properties as functions of pressure and temperature. The presented
functions generally ensure a computation accuracy not worse than
1.3 percent of the current thermodynamic table values. They cover a
range of pressure from atmospheric up to 15 MPa which is sufficient for
the majority of normal and abnormal operating conditions. In developing
the approximation formulas an emphasis has been placed on nonlinear
functional approximation rather than on nonlinear regression of power
series expansions. The approximations are sufficiently simple that they
may be effectively used with programmable calculators, as well as with
micro computers.

10th Annual Symposium on Simulation of Reactor Dynamics and Plant Control
April 9-10, 1984, Saint John, New Brunswick

## 1.0     INTRODUCTION

Heavy water thermodynamic properties are used extensively in many areas
of CANDU PHWR analysis. These properties are often calculated by
commonly used linear interpolation algorithms applied to thermodynamic
tables stored in computer memory.

Such an approach, while being direct and relatively simple, is not
necessarily the most efficient. Storage of the tables can occupy a large
amount of computer memory and the process of inputting the table data
into a computer is time-consuming, prone to input errors and difficult
for verification. Furthermore, the linear interpolation algorithms,
which themselves are quite simple, require a searching algorithm for
selecting proper numbers from the table. Such searching algorithms,
particularly in case of large, two-dimensional (pressure and temperature)
property tables used for frequent calculations, can result in substantial
use of computer time.

For the purpose of system analysis an accuracy of one percent in the
computation of these properties is usually quite satisfactory.

Therefore there is no need for more accurate calculation of the heavy water thermodynamic properties, particularly when employed in codes used for approximate, scoping analysis.

The purpose of this paper is to demonstrate some very simple algorithms which enable rapid calculation of $D_2O$ thermodynamical properties without employing the vast input data tables. During development of these algorithms an emphasis has been placed on nonlinear functional approximation rather than on nonlinear regression of power series expansions. Using this approach a more uniform accuracy over the whole range of independent variables has been achieved.

The approximations are simple enough to be effectively used with microcomputers as well as with programmable calculators. The range of validity of both pressure and temperature variations is sufficient for the majority of normal and abnormal operating conditions applicable to CANDU reactors. An approximation accuracy is usually better than 1.3 percent which is more than adequate for the kind of simulation tasks specified.

## 2.0     NONLINEAR FUNCTIONAL APPROXIMATION APPROACH

An emphasis has been placed on utilization of simple nonlinear functions of an a-priori given form rather than on employing the commonly used methods of linear and nonlinear regression of power series expansions. This is justified by a desire to obtain approximation forms which are very simple and easy for computer implementations. Also, a preference was given to the approach of "almost exact matching to table data" instead of minimizing a mean square error of the approximation.

In a case of regression-type approximation, particularly when utilizing low-order models, the best mean-square error fittings lead to approximations with relatively small mean-square errors but often with substantial local deviations from the given data. Utilization of higher-order regressional models usually corrects this problem but leads to more complicated models. Moreover, the regression models tend to deviate very rapidly from the given table values when used outside the range used in the regression. This tendency is particularly evident for higher order nonlinear regression models.

The approach used in this paper is based on detailed analysis of the given data tables and on finding simple nonlinear functions which provide a satisfactory fit to the given data rather than on minimizing a mean-square error of the approximation. There is no universal, algorithmic formula which would do this task automatically. Instead, each physical property to be approximated has been analyzed separately. A graphical representation of the data often helped in finding an adequate approximation function. Wherever possible, normalized general exponential functions were used and then re-scaled to yield good matching.

Having chosen the type of approximation function, some of its parameters were correlated with temperature and pressure to ensure adequate approximation accuracy over a pre-defined region of the independent variables.

In order to maintain the computational simplicity of the approximation formula, the ranges of temperature and pressure variations were often partitioned into smaller sub-regions. Then, for the each sub-region separate correlations for individual parameters of the employed approximation function have been developed. Computational iterative procedures were often used. For some of the $D_2O$ properties, correlations with pressure are neglected in the pressure region between 0.1 and 15 MPa and the resulting accuracy of approximation remained satisfactory.

It should be stressed that the approximation forms for the $D_2O$ thermodynamical properties described below ensure an adequate accuracy achieved by very modest and simple means. At the same time the presented formulas are simple enough to be effectively used even in hand calculations with programmable calculators.

## 3.0    APPROXIMATION TO $D_2O$ THERMODYNAMIC PROPERTIES

The AECL tables of thermodynamic properties of heavy water, Reference 1, have been used as a reference source of data. The range of temperature and pressure variations considered are correspondingly, about (27-350)°C and (0.1-15) MPa.

### 3.1    Specific Volume-Liquid Phase at Saturation Conditions

An approximation $\hat{v}_f$ to the $D_2O$ specific volume-liquid phase $v_f$ given in Reference 1, Table 2 for saturation conditions, is given below as a simple linear function of pressure P.

Approximation algorithm:

$$\hat{v}_f = 9.602 \times 10^{-4} + 5.11333 \times 10^{-5} P, \quad \text{for } P < 2.3 \text{ MPa};$$

$$\hat{v}_f = 1.00938 \times 10^{-3} + 3.05429 \times 10^{-5} P, \quad \text{for } P \geqslant 2.3 \text{ MPa};$$

where:    $P$    =    saturation pressure, [MPa]

            $\hat{v}_f$    =    approximation to specific volume-fluid, [m³/kg]

Recommended range of use: (0.1-14)MPa with accuracy $\epsilon$ not worse than 2.56 percent.

Accuracy of the approximation formula is shown in Table 1 below and in Figure 3.1.

<div align="center">

TABLE 1:  Accuracy of the Approximation Formula
for $D_2O$ Specific Volume-Liquid Phase

</div>

| P, [MPa] | $v_f$, [m³/kg] | $\hat{v}_f$, [m³/kg] | $\epsilon = \dfrac{v_f - \hat{v}_f}{v_f}$, [%] |
|---|---|---|---|
| 0.1 | 0.0009412 | 0.0009653 | -2.56 |
| 0.2 | 0.0009568 | 0.0009704 | -1.42 |
| 0.5 | 0.0009858 | 0.0009858 | 0 |
| 0.8 | 0.0010060 | 0.0010011 | +0.49 |
| 1 | 0.0010173 | 0.0010113 | +0.59 |
| 1.5 | 0.0010416 | 0.0010369 | +0.45 |
| 2 | 0.0010625 | 0.0010625 | 0 |
| 2.5 | 0.0010813 | 0.0010857 | -0.41 |
| 3 | 0.0010989 | 0.0011010 | -0.19 |
| 4 | 0.0011317 | 0.0011316 | +0.01 |
| 5 | 0.0011626 | 0.0011621 | +0.04 |
| 8 | 0.0012529 | 0.0012537 | -0.07 |
| 10 | 0.0013158 | 0.0013148 | +0.08 |
| 12 | 0.0013845 | 0.0013759 | +0.62 |
| 13 | 0.0014222 | 0.0014064 | +1.11 |
| 15 | 0.0015077 | 0.0014675 | +2.66 |

## 3.2    Specific Volume-Vapour Phase at Saturation Conditions

An estimate $\hat{v}_g$ of $D_2O$ specific volume-vapour phase is obtained by employing linear and second-order parabolic functions of pressure P as approximations to the inverse of specific volume (vapour) at saturation conditions.

Approximation algorithm:

$$(\hat{v}_g)^{-1} = 5.5468\ P + 0.1073, \qquad\qquad \text{for } 0.1\ \text{MPa} \leqslant P < 3\ \text{MPa};$$

$$(\hat{v}_g)^{-1} = 0.16511(P)^2 + 4.41083\ P + 2.02911, \quad \text{for } 3\ \text{MPa} \leqslant P \leqslant 14\ \text{MPa};$$

where:  $\hat{v}_g$  =  approximation to $D_2O$ specific volume-vapour phase, $[m^3/kg]$

P  =  saturation pressure, [MPa].

Recommended range of use:  (0.1-14)MPa with accuracy $\epsilon$ not worse than 2.9 percent.

The approximation accuracy is indicated in the Table 2 and Figure 3.2.

TABLE 2:  Accuracy of the Approximation for
$D_2O$ Specific Volume-Vapour Phase

| P, [MPa] | $v_g$, $[m^3/kg]$ | $\hat{v}_g$, $[m^3/kg]$ | $\epsilon = \dfrac{v_g - \hat{v}_g}{v_g}$, [%] |
|---|---|---|---|
| 0.1 | 1.51073 | 1.51073 | 0 |
| 0.2 | 0.79885 | 0.82196 | -2.89 |
| 0.5 | 0.33750 | 0.34714 | -2.86 |
| 1 | 0.174741 | 0.17686 | -1.22 |
| 1.5 | 0.118279 | 0.11866 | -0.3 |
| 2 | 0.089343 | 0.08928 | +0.07 |
| 3 | 0.059710 | 0.059710 | 0 |
| 4 | 0.044519 | 0.044815 | -0.66 |
| 5 | 0.035233 | 0.035447 | -0.61 |
| 8 | 0.020935 | 0.020884 | +0.24 |
| 10 | 0.016007 | 0.015962 | +0.28 |
| 12 | 0.012634 | 0.012701 | -0.53 |
| 13 | 0.011306 | 0.011458 | -1.35 |
| 14 | 0.010147 | 0.010401 | -2.51 |
| 15 | 0.009121 | 0.009493 | -4.08 |

Note that within a narrower pressure range, between 1 MPa and 12.5 MPa the accuracy is better than 1.25 percent, which is quite satisfactory.
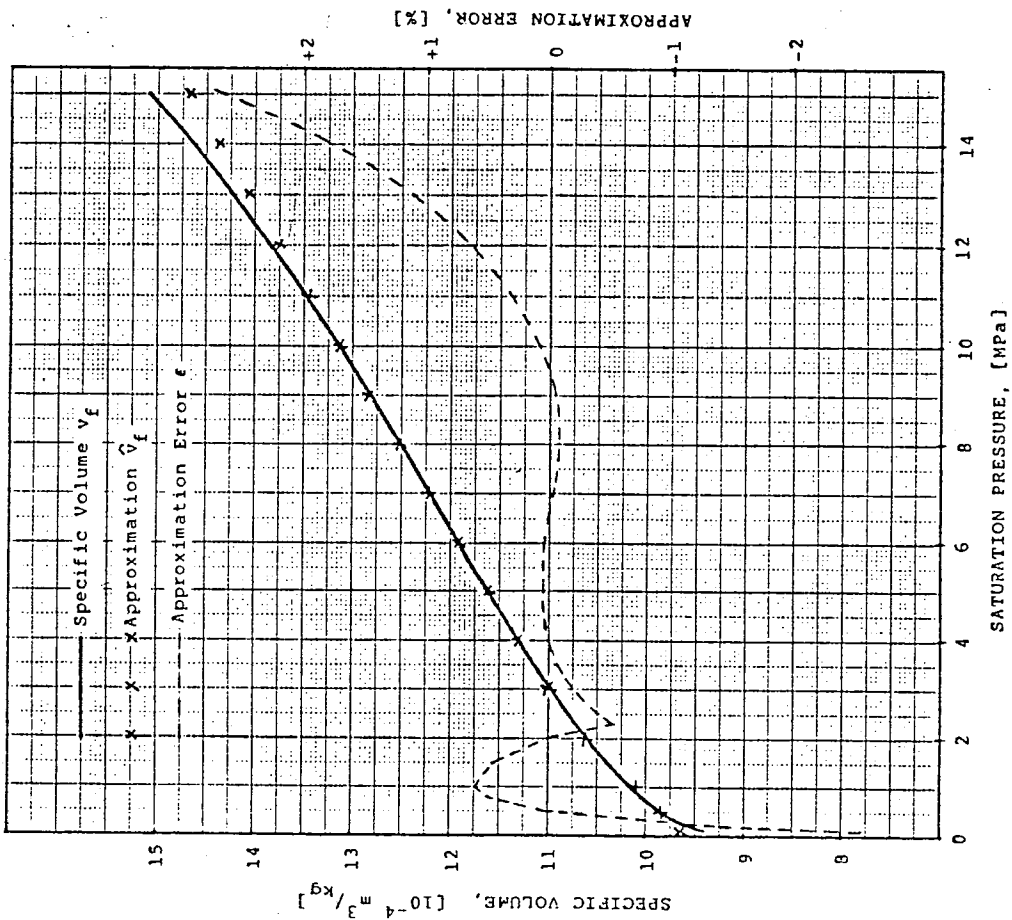
FIGURE 3.2

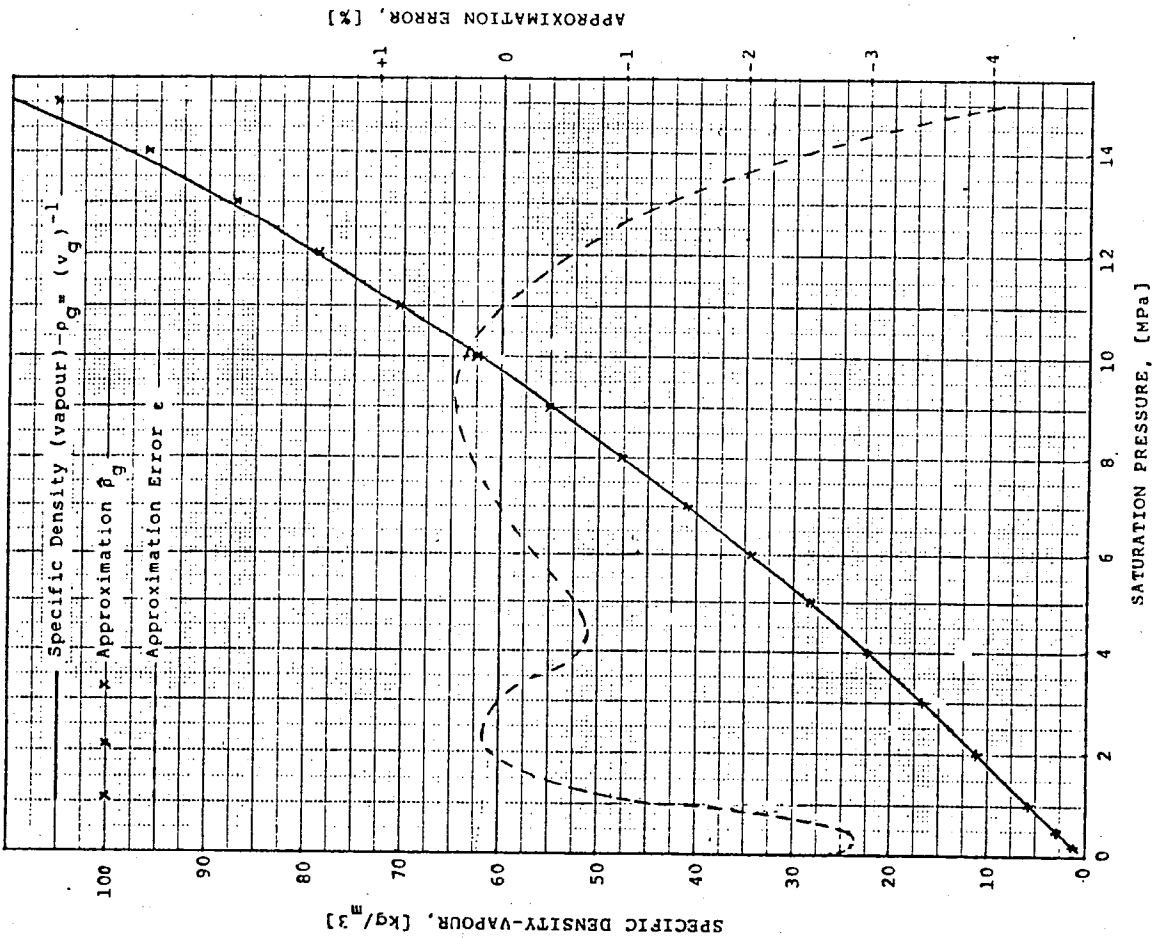Approximation of $D_2O$ Specific Volume (vapour) at Saturation Conditions



Figure 3.1

Approximation to $D_2O$ Specific Volume (liquid) at Saturation Conditions

### 3.3  Saturation Temperature

An exponential function of pressure P, with pressure variations
normalized to 10 MPa is used to get an approximation formula to the $D_2O$
saturation temperature $T_{SAT}$.

Approximation algorithm:

$$\hat{T}_{SAT} = 310.06 \left(\frac{P}{10}\right)^a$$

$$a = \begin{cases} 0.241 \text{ for } P < 0.3 \text{ MPa} \\ 0.236 \text{ for } P > 0.3 \text{ MPa} \end{cases}$$

where: $\hat{T}_{SAT}$ = approximation to $D_2O$ saturation temperature, [°C]

$P$ = pressure, [MPa]

Recommended range of use: (0.1-15)MPa with accuracy better than
1.1 percent.

Accuracy of the approximation formula is presented in Table 3 and in the
attached Figure 3.3.

TABLE 3:  Accuracy of the Approximation to $D_2O$ Saturation Temperature

| P, [MPa] | $T_{SAT}$, [°C] | $\hat{T}_{SAT}$, [°C] | $\epsilon = \dfrac{T_{SAT} - \hat{T}_{SAT}}{T_{SAT}}$, [%] |
|---|---|---|---|
| $5 \times 10^{-2}$ | 82.99 | 86.48 | -4.21 |
| 0.1 | 101.05 | 102.20 | -1.14 |
| 0.2 | 121.41 | 120.78 | +0.52 |
| 0.5 | 152.66 | 152.90 | -0.16 |
| 1 | 180.38 | 180.07 | +0.17 |
| 1.5 | 198.58 | 198.15 | +0.21 |
| 2 | 212.51 | 212.07 | +0.20 |
| 3 | 233.75 | 233.37 | +0.16 |
| 5 | 263.51 | 263.27 | +0.09 |
| 8 | 294.24 | 294.15 | +0.03 |
| 10 | 310.06 | 310.06 | 0 |
| 13 | 329.69 | 329.87 | -0.05 |
| 15 | 340.86 | 341.20 | -0.10 |

It is worth to point out that within the pressure range from 0.5 MPa up
to 15 MPa the accuracy of approximation is very good, namely better than
0.21 percent.

## 3.4    Enthalpy of Liquid Phase at Saturation Conditions

Exponential functions of the saturation pressure P, normalized to three pressure levels:  1.5 MPa, 5 MPa and 10 MPa are employed.

Approximation algorithm:

$$\hat{h}_f = 819.15 \left(\frac{P}{1.5}\right)^{0.255}, \text{ for } 50 \text{ kPa} \leqslant P < 1.5 \text{ MPa};$$

$$\hat{h}_f = 1112.0 \left(\frac{P}{5}\right)^{0.256}, \text{ for } 1.5 \text{ MPa} \leqslant P < 5.2 \text{ MPa};$$

$$\hat{h}_f = 1350.14 \left(\frac{P}{10}\right)^{0.283}, \text{ for } 5.2 \text{ MPa} \leqslant P < 15 \text{ MPa};$$

where:  $\hat{h}_f$ = approximation to saturation enthalpy of $D_2O$ liquid phase, [kJ/kg].

P = saturation pressure, [MPa].

Recommended range of use:  (0.1-14)MPa, with accuracy not worse than 1.2 percent.

Accuracy of the approximation is illustrated in Table 4 below and in the attached Figure 3.4.

TABLE 4:  Accuracy of the Approximation to $D_2O$
Liquid Phase Enthalpy at Saturation Conditions

| P, [MPa] | $h_f$, [kJ/kg] | $\hat{h}_f$, [kJ/kg] | $\epsilon = \dfrac{h_f - \hat{h}_f}{h_f}$, [%] |
|---|---|---|---|
| $5 \times 10^{-2}$ | 334.16 | 344.11 | -2.98 |
| 0.1 | 409.49 | 410.64 | -0.28 |
| 0.2 | 494.14 | 490.03 | +0.83 |
| 0.5 | 624.36 | 619.01 | +0.86 |
| 1 | 741.20 | 738.69 | +0.34 |
| 1.5 | 819.15 | 819.15 | 0 |
| 2 | 879.75 | 879.49 | +0.03 |
| 3 | 974.14 | 975.69 | -0.16 |
| 5 | 1112.0 | 1112.0 | 0 |
| 6 | 1167.75 | 1168.41 | -0.06 |
| 8 | 1264.90 | 1267.52 | -0.21 |
| 10 | 1350.14 | 1350.14 | 0 |
| 12 | 1428.48 | 1421.63 | +0.48 |
| 14 | 1503.19 | 1485.02 | +1.21 |
| 15 | 1540.10 | 1514.30 | +1.68 |

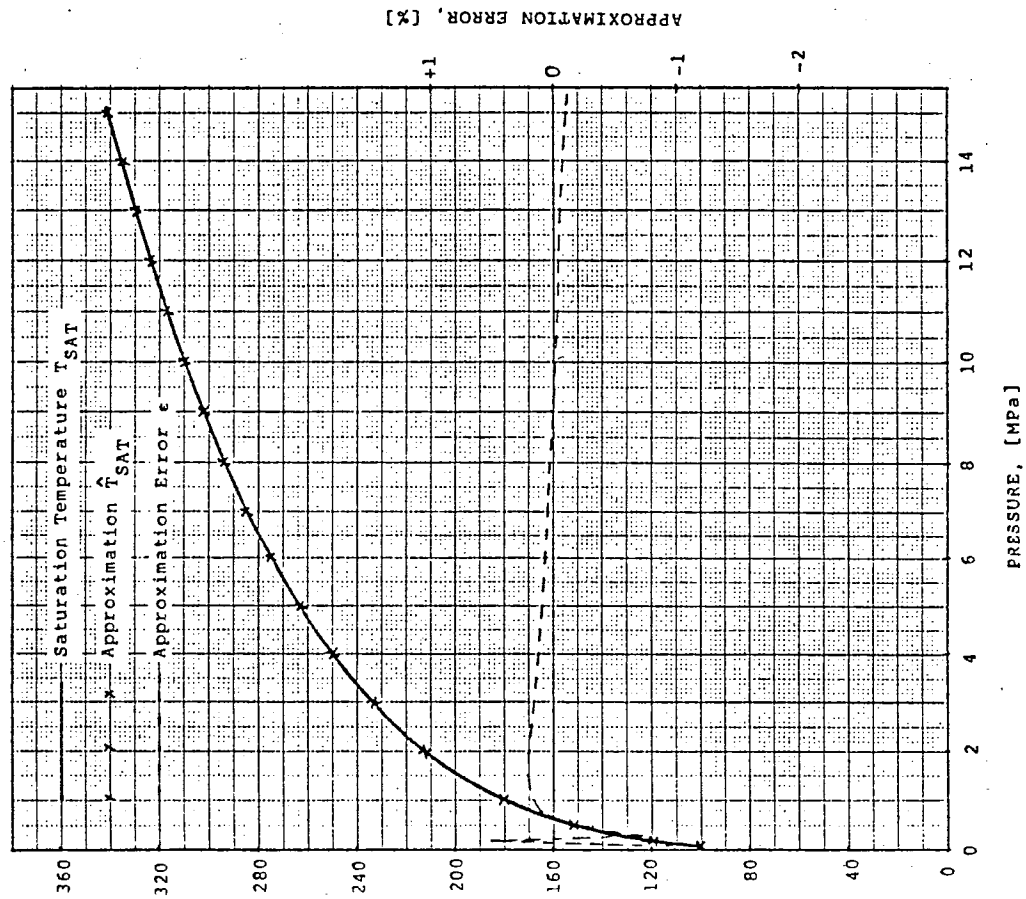Note that in the pressure range between 1 MPa and 11 MPa the approximation accuracy is better than 0.35 percent.

0776b

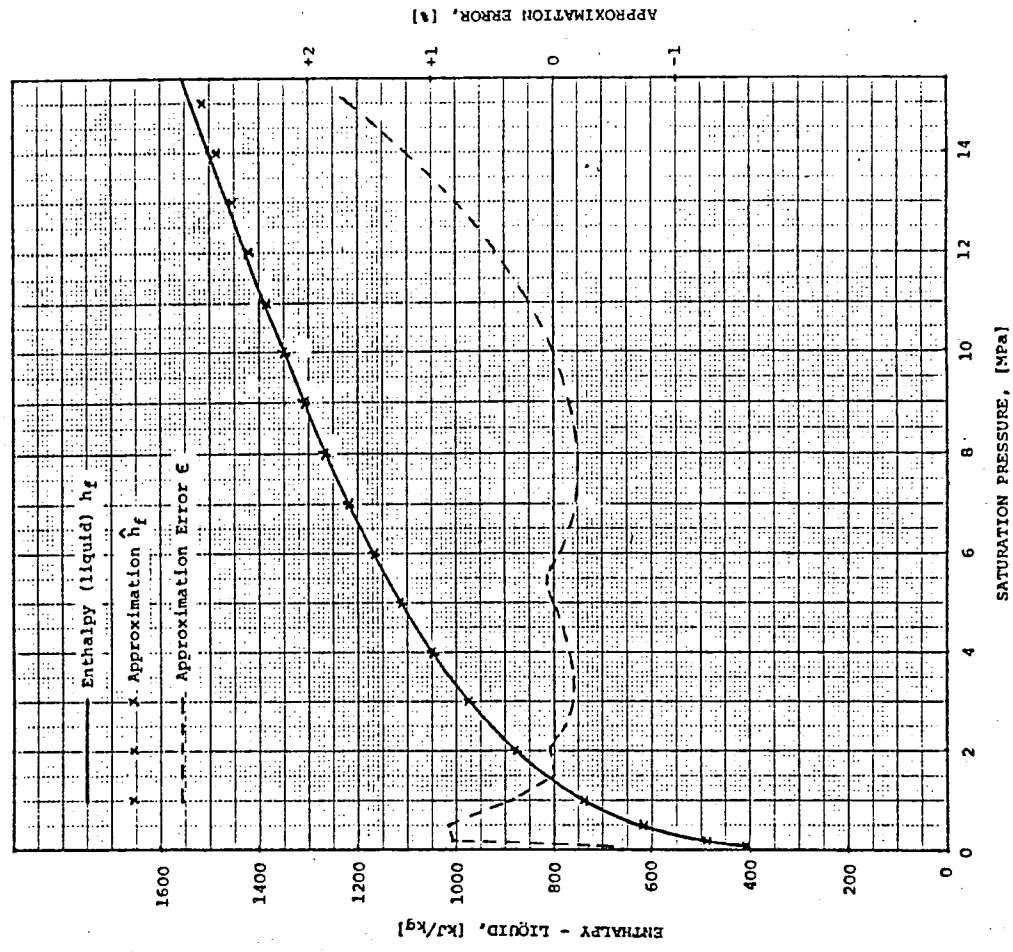FIGURE 3.4
Approximation to $D_2O$ Saturation Enthalpy – Liquid Phase



FIGURE 3.3
Approximation to $D_2O$ Saturation Temperature

### 3.5 Enthalpy of Evaporation

For approximation to the $D_2O$ evaporation enthalpy $h_{fg}$, normalized exponential functions and simple linear relation are used.

The approximation algorithm is:

$$\hat{h}_{fg} = 2202.7 - 879.4 \left(\frac{P}{7.5}\right)^{\frac{1}{a}}, \quad \text{for } 50 \text{ kPa} \leqslant P < 2.5 \text{ MPa};$$

$$a = 2.27$$

$$\hat{h}_{fg} = 2181.2 - 857.9 \left(\frac{P}{7.5}\right)^{\frac{1}{a}}, \quad \text{for } 2.5 \text{ MPa} \leqslant P < 7 \text{ MPa};$$

$$a = 2.10$$

$$\hat{h}_{fg} = 1754.8 - 57.53 \, P, \quad \text{for } 7 \text{ MPa} \leqslant P \leqslant 15 \text{ MPa};$$

where:   $\hat{h}_{fg}$ =   enthalpy of evaporation, [kJ/kg]

   $P$ =   saturation pressure, [MPa]

Recommended range of use:   (0.05-15)MPa with accuracy better than 0.8 percent.

The accuracy of approximation is shown in Table 5 below and in Figure 3.5.

TABLE 5:   Accuracy of Approximation to $D_2O$ Evaporation Enthalpy

| $P$, [MPa] | $h_{gf}$, [kJ/kg] | $\hat{h}_{gf}$, [kJ/kg] | $\epsilon = \dfrac{h_{gf} - \hat{h}_{gf}}{h_{gf}}$, [%] |
|---|---|---|---|
| $1 \times 10^{-2}$ | 2210.3 | 2155.1 | +2.5 |
| $2 \times 10^{-2}$ | 2174.0 | 2138.1 | +1.65 |
| $5 \times 10^{-2}$ | 2119.3 | 2106.0 | +0.63 |
| 0.1 | 2071.4 | 2071.4 | 0 |
| 0.2 | 2015.7 | 2024.6 | −0.44 |
| 0.5 | 1924.2 | 1936.0 | −0.61 |
| 1 | 1834.2 | 1840.7 | −0.35 |
| 1.5 | 1768.9 | 1769.9 | −0.06 |
| 2.5 | 1667.6 | 1672.8 | −0.31 |
| 3 | 1624.8 | 1626.6 | −0.11 |
| 5 | 1478.7 | 1473.9 | +0.32 |
| 7 | 1353.1 | 1352.1 | +0.07 |
| 10 | 1178.9 | 1179.5 | −0.05 |
| 12 | 1064.4 | 1064.4 | 0 |
| 13 | 1006.2 | 1006.9 | −0.07 |
| 14 | 946.6 | 949.4 | −0.29 |
| 15 | 884.9 | 891.9 | −0.79 |

Within a narrower pressure range, from about 1 MPa up to 14 MPa the obtained accuracy is better than 0.35 percent.

## 3.6    Subcooled Liquid Enthalpy

Simple linear functions of temperature T are used for the approximation.
Variations with pressure P are neglected due to fact that subcooled
enthalpy only slightly varies with pressure. The coefficients of the
approximation function are calculated at the reference pressure
P = 10.0 MPa.

Approximation algorithm:

$$\hat{h}_{SUB} = 4.1615 \ (T-1.2494), \qquad \text{for } 25°C \leqslant T < 100°C;$$
$$\hat{h}_{SUB} = 4.2199 \ (T-3.436), \qquad \text{for } 100°C \leqslant T < 225°C;$$
$$\hat{h}_{SUB} = 4.7733 \ (T-29.992), \qquad \text{for } 225°C \leqslant T < 310.1°C;$$

where:  $\hat{h}_{SUB}$ = approximation to $D_2O$ subcooled enthalpy, [kJ/kg]
        T = subcooled temperature, [°C]

Recommended range of use:   (25-310)°C with accuracy not worse than
1 percent at pressure P = 10.0 MPa.

Accuracy of the approximation at P = 10.0 MPa is given in Table 6 below
and in Figure 3.6

TABLE 6:   Accuracy of the Approximation to
$D_2O$ Subcooled Enthalpy at P = 10.0 MPa

| T, [°C] | $h_{SUB}$, [kJ/kg] | $\hat{h}_{SUB}$, [kJ/kg] | $\epsilon = \dfrac{h_{SUB}-\hat{h}_{SUB}}{h_{SUB}}$, [%] |
|---|---|---|---|
| 25 | 98.3 | 98.8 | -0.51 |
| 50 | 203.5 | 202.9 | +0.30 |
| 80 | 328.8 | 327.7 | +0.34 |
| 100 | 411.8 | 407.5 | +1.04 |
| 140 | 577.1 | 576.3 | +0.14 |
| 180 | 743.7 | 745.1 | -0.19 |
| 200 | 828.2 | 829.5 | -0.16 |
| 220 | 914.6 | 913.9 | +0.08 |
| 260 | 1094.5 | 1097.9 | -0.31 |
| 300 | 1293.7 | 1288.8 | +0.38 |
| 310 | 1349.8 | 1336.6 | +0.98 |

Observe that pressure reduction at constant temperatures (below
saturation point) results in relatively insignificant variations of the
subcooled enthalpy. For example, at P = 2 MPa and T = 40°C the subcooled
enthalpy is, according to Reference 1, h = 155.0 kJ/kg. Reducing the
pressure down to 0.1 MPa yields h = 153.4 kJ/kg. In both the cases our
approximation yields value of 161.3 kJ/kg with an accuracy of 4.1 percent
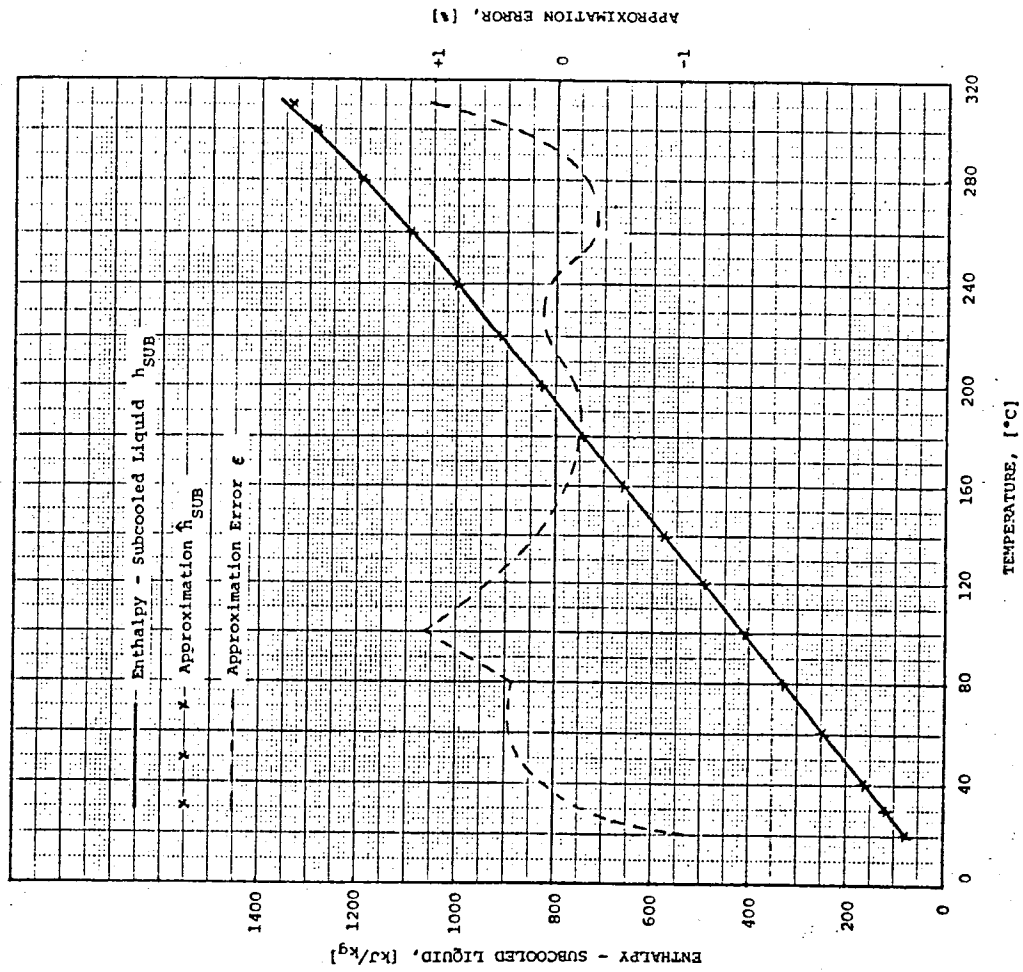and 5.1 percent, correspondingly.

APPROXIMATION ERROR, [%]

Enthalpy – Subcooled Liquid $h_{SUB}$
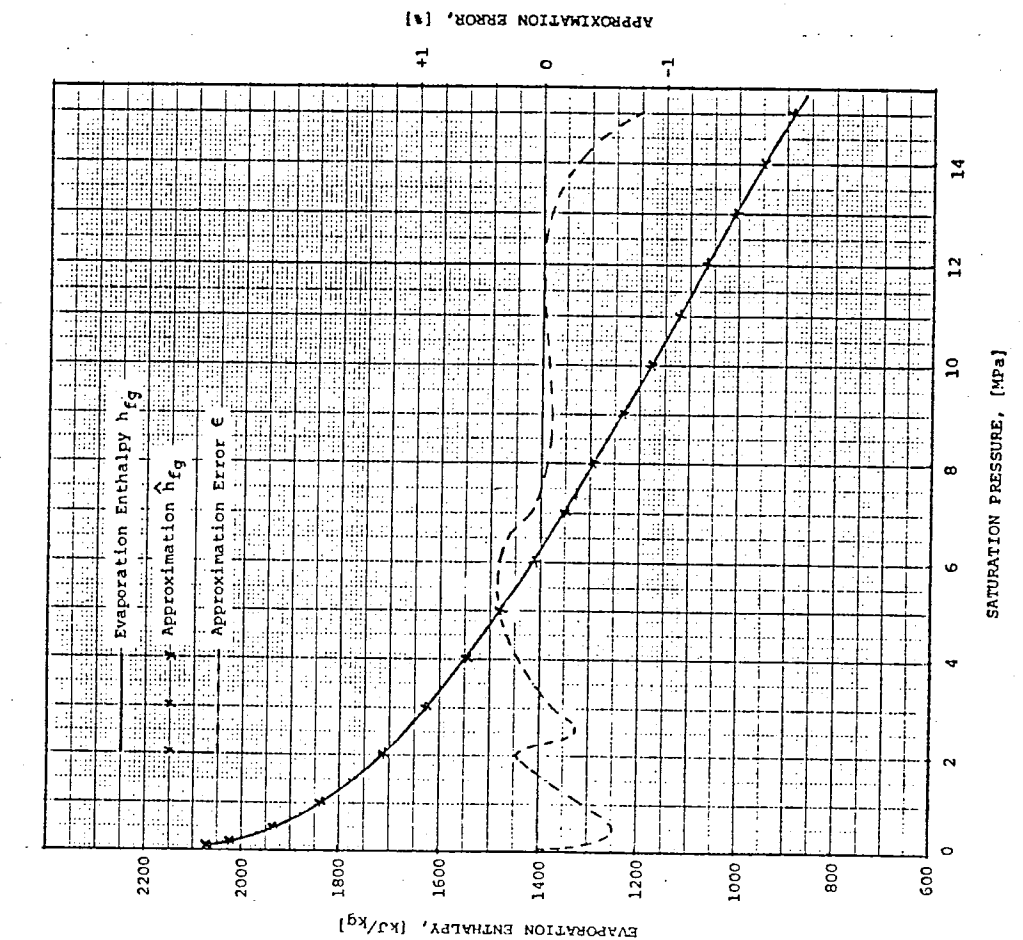Approximation $\hat{h}_{SUB}$
Approximation Error $\epsilon$

ENTHALPY – SUBCOOLED LIQUID, [kJ/kg]

TEMPERATURE, [°C]

FIGURE 3.6
Approximation to Specific Enthalpy of $D_2O$ – Subcooled Liquid, at Pressure P = 10 MPa



APPROXIMATION ERROR, [%]

Evaporation Enthalpy $h_{fg}$
Approximation $\hat{h}_{fg}$
Approximation Error $\epsilon$

EVAPORATION ENTHALPY, [kJ/kg]

SATURATION PRESSURE, [MPa]

FIGURE 3.5
Approximation to $D_2O$ Evaporation Enthalpy

## 3.7    Specific Heat of Liquid Phase

Normalized exponential and parabolic functions in temperature T are used for the approximation.  Variations with pressure have been neglected.

Coefficients of the approximation are correlated at pressure P = 10.0 MPa.

Approximation algorithm:

$$\hat{C}_{pf} = 4.205, \qquad\qquad\qquad \text{for } 20°C \leq T < 45°C;$$

$$\hat{C}_{pf} = 4.213 - 0.0017\tau + 8.75 \times 10^{-6}(\tau)^2, \qquad \text{for } 45°C \leq T < 130°C;$$

$$\tau = T - 140$$

$$\hat{C}_{pf} = 4.131 - 2.333 \times 10^{-4}\tau + 3.25 \times 10^{-5}(\tau)^2, \qquad \text{for } 130°C \leq T < 255°C;$$

$$\tau = T - 130$$

$$\hat{C}_{pf} = 4.269 + 0.881 \left(\frac{T-200}{90}\right)^{1.95}, \qquad \text{for } 255°C \leq T < 290°C;$$

$$\hat{C}_{pf} = 4.130 + 1.691 \left(\frac{T-120}{190.1}\right)^{4.6}, \qquad \text{for } 290°C \leq T \leq 310.1°C;$$

where:    $\hat{C}_{pf}$ = approximation to specific heat of $D_2O$ liquid phase, $\left[\frac{kJ}{kg.°K}\right]$

$\phantom{where:}$   T   = temperature, [°C]

Recommended range of use:    (20-310)°C with accuracy not worse than 0.41 percent at constant pressure P = 10.0 MPa.

Accuracy of this approximation is illustrated in Table 7 below and in Figure 3.7.

TABLE 7: Accuracy of the Approximation to Specific Heat
of $D_2O$ Liquid Phase at Pressure P = 10.0 MPa

| T, [°C] | $C_{pf}$, [kJ/kg] | $\hat{C}_{pf}$, [kJ/kg] | $\epsilon = \dfrac{C_{pf}-\hat{C}_{pf}}{C_{pf}}$, [%] | $\lvert\epsilon\rvert_p^{Max}$, [%] |
|---|---|---|---|---|
| 20 | 4.208 | 4.205 | +0.07 | 0.87 |
| 30 | 4.211 | 4.205 | +0.14 | 0.83 |
| 50 | 4.197 | 4.197 | 0 | 0.55 |
| 60 | 4.186 | 4.183 | +0.08 | 0.57 |
| 80 | 4.161 | 4.159 | +0.05 | 0.53 |
| 100 | 4.140 | 4.143 | −0.06 | 0.43 |
| 120 | 4.130 | 4.133 | −0.07 | 0.48 |
| 150 | 4.145 | 4.139 | +0.14 | 0.82 |
| 180 | 4.204 | 4.201 | +0.08 | 0.92 |
| 200 | 4.269 | 4.274 | −0.12 | 0.86 |
| 230 | 4.419 | 4.433 | −0.31 | 0.98 |
| 250 | 4.571 | 4.571 | 0 | 1.55 |
| 270 | 4.793 | 4.809 | −0.33 | 1.25 |
| 290 | 5.150 | 5.141 | +0.17 | 1.48 |
| 310 | 5.821 | 5.821 | 0 | 0 |

$\lvert\epsilon\rvert_p^{Max}$ = maximum absolute value of the approximation error over
whole range of pressure variations between 100 kPa and 10 MPa,
restricted to liquid phase.

Note that the maximum possible error of approximation $\lvert\epsilon\rvert_p^{Max}$ caused by
pressure variations does not exceed 1.6 percent which is quite
satisfactory, keeping in mind the simplicity of the approximation
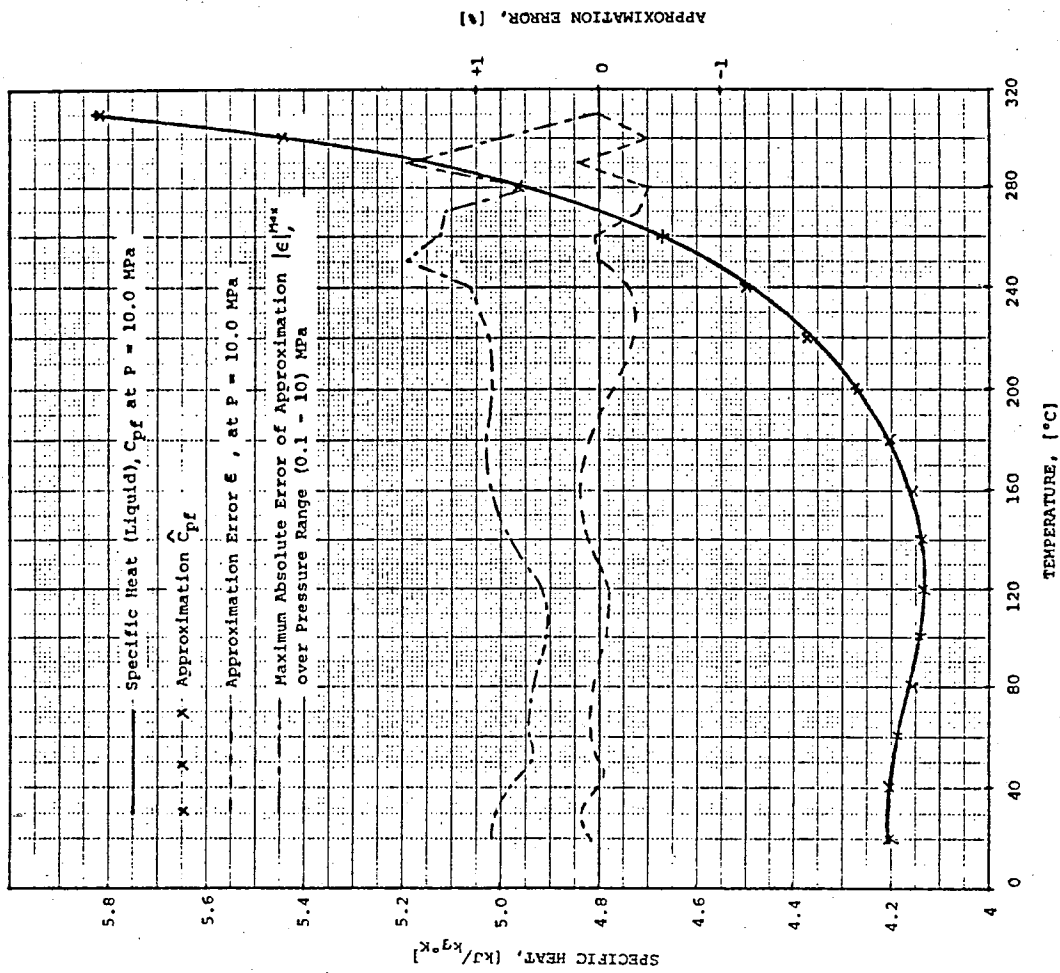algorithm.

FIGURE 3.7

Approximation to D₂O Specific Heat - Liquid Phase, at Pressure P = 10 MPa

### 3.8    Dynamic Viscosity

Heavy water dynamic viscosity $\mu = \nu\rho$   for liquid and vapour phases, re-calculated from the kinematic viscosity in Reference 1, Table 10, while accommodating for pressure and temperature variations of density $\rho$ , is shown in the following Table 8.

Based on this table, simple approximations to liquid phase dynamic viscosity $\mu_f$ and vapour phase dynamic $\mu_g$ have been developed.

### 3.8.1    Dynamic Viscosity of Liquid Phase

A combination of exponential and hyperbolic functions is used for the approximation to dynamic viscosity $\mu_f$.

The approximation algorithm is:

$$\hat{\mu}_f = [25(10)^x + 0.1\beta x\, P];$$

$$x = \frac{250}{127+T}, \qquad \beta = 5$$

where: $\hat{\mu}_f$ = approximation to $D_2O$ dynamic viscosity (liquid), in $[10^{-6} \frac{kg}{m.s}]$

    T = temperature, [°C]
    P = pressure, [MPa]
    $\beta$ = correction factor

Recommended range of use:  from 5°C up to saturation temperature, with accuracy not worse than 4.7 percent at constant pressure of 10 MPa.

The algorithm ensures good accuracy within the range of nominal operating conditions of a typical CANDU-PHW reactor outlet header, that is in the vicinity of P = 9.5 MPa and T = 290°C.  The accuracy deteriorates with decreasing temperature T, particularly in the range of (90-190)°C but even there it is not worse than 4.7 percent.  This is illustrated in Table 9, as follows:

TABLE 8: D$_2$O Dynamic Viscosity $\mu = \nu\rho$, in $[10^{-6} \frac{kg}{m.s}]$

| T[°C] | 3.85 | 27 | 77 | 127 | 177 | 227 | 277 | 327 | 352 | 377 | 402 | 427 | 477 | 527 |
|---|---|---|---|---|---|---|---|---|---|---|---|---|---|---|
| 0.1 | 2046.43 | 1048.13 | 432.08 | 13.536 | 15.794 | 17.745 | 19.786 | 21.875 | 22.936 | 24.004 | 25.075 | 26.166 | 28.366 | 30.607 |
| 1 | 2045.13 | 1048.16 | 432.26 | 255.43 | 174.52 | 17.512 | 19.627 | 21.772 | 22.877 | 23.975 | 25.076 | 26.184 | 28.415 | 30.682 |
| 2.5 | 2043.39 | 1048.19 | 432.76 | 255.96 | 175.01 | 133.27* | 19.346 | 21.612 | 22.765 | 23.925 | 25.071 | 26.208 | 28.486 | 30.776 |
| 5 | 2040.34 | 1048.14 | 433.45 | 256.70 | 175.32 | 131.93 | 18.848 | 21.353 | 22.625 | 23.857 | 25.076 | 26.275 | 28.625 | 30.965 |
| 7.5 | 2038.82 | 1048.35 | 434.18 | 257.47 | 175.95 | 132.68 | 105.62 | 21.120 | 22.512 | 23.841 | 25.126 | 26.364 | 28.792 | 31.181 |
| 10 | 2034.44 | 1048.17 | 434.87 | 258.25 | 177.05 | 133.31 | 106.60 | 20.943 | 22.440 | 23.867 | 25.199 | 26.485 | 28.950 | 31.406 |
| 15 | 2029.63 | 1048.20 | 436.21 | 259.77 | 178.48 | 134.78 | 108.15 | 83.54 | 22.732 | 24.168 | 25.530 | 26.839 | 29.382 | 31.940 |
| 20 | 2023.45 | 1048.08 | 437.59 | 261.29 | 179.89 | 136.12 | 109.64 | 86.47 | 72.15 | 25.536 | 26.329 | 27.483 | 29.958 | 32.60 |
| 25 | 2017.24 | 1047.92 | 438.85 | 262.80 | 181.20 | 137.44 | 111.07 | 88.88 | 77.20 | 54.80 | 28.406 | 28.653 | 30.749 | 33.427 |

PRESSURE, [MPa]

*) This value was calculated for liquid saturation point at T = 224°C, P = 2.5 MPa, based on linear approximation of kinematic viscosity with respect to P and T.

TABLE 9: Approximation Accuracy for Dynamic Viscosity of
$D_2O$-Liquid Phase at Pressure P ≐ 10.0 MPa

| T, [°C] | $\mu_f$, [$10^{-6} \frac{kg}{m.s}$] | $\hat{\mu}_f$, [$10^{-6} \frac{kg}{m.s}$] | $\epsilon = \frac{\mu_f - \hat{\mu}_f}{\mu_f}$, [%] |
|---|---|---|---|
| 3.85 | 2034.44 | 2044.37 | -0.49 |
| 26.9 | 1048.17 | 1060.98 | -1.22 |
| 76.9 | 434.87 | 427.89 | +1.84 |
| 126.9 | 258.25 | 246.24 | +4.65 |
| 177 | 177.05 | 170.29 | +3.82 |
| 227 | 133.31 | 130.69 | +1.97 |
| 277 | 106.60 | 107.06 | -0.43 |

When reducing pressure to 0.1 MPa, the inaccuracy of approximation to $\mu_f$ does not exceed 5.3 percent which is still acceptable. Note that the estimates of $\mu_f$ are needed mainly in computation of the Reynolds and Prandtl numbers and there is no need to calculate these numbers very accurately.

Nevertheless, the accuracy of this approximation can be substantially improved by correlating the correction factor $\beta$ with temperature T and pressure P. Regular patterns of that correlation can be observed but their description is beyond the scope of this paper.

### 3.8.2 Dynamic Viscosity of Vapour Phase

A linear function of temperature T with coefficients correlated with pressure P has been used for the approximation.

The approximation algorithm is:

$$\hat{\mu}_g = aT+b;$$

$$\left.\begin{array}{ll} a = (4.212 + 0.148\ P) \times 10^{-2} \\ b = 8.25 - 0.6428\ P \end{array}\right\} \text{ for } 100\ \text{kPa} \leqslant P < 2.5\ \text{MPa};$$

$$\left.\begin{array}{ll} a = (4.31 + 0.108\ P) \times 10^{-2} \\ b = 8.133 - 0.633\ P + 0.0149(P)^2 \end{array}\right\} \text{ for } 2.5\ \text{kPa} \leqslant P < 10.0\ \text{MPa};$$

$$\left.\begin{array}{ll} a = (5.27 + 0.012\ P) \times 10^{-2} \\ b = 3.027 - 0.0268\ P; \end{array}\right\} \text{ for } 10\ \text{MPa} \leqslant P \leqslant 15\ \text{MPa};$$

where: $\hat{\mu}_g$ = approximation to $D_2O$ dynamic viscosity (vapour), in [$10^{-6} \frac{kg}{m.s}$]

$\quad$ T = temperature (above saturation value), [°C]
$\quad$ P = pressure, [MPa]
$\quad$ a,b = linear coefficients

TABLE 10: Accuracy of Approximation to Dynamic Viscosity of $D_2O$ - Vapour Phase, $\eta_g$

| $\eta_g$ [$10^{-6}$ kg/m.s] / Pressure [MPa] | 76.9 | 126.9 | 177 | 227 | 277 | 327 | 352 | 377 | 402 | 427 | 477 | 527 |
|---|---|---|---|---|---|---|---|---|---|---|---|---|
| 0.1 | | -0.1%<br>13.550<br>13.536 | +0.8%<br>15.667<br>15.794 | -0.2%<br>17.781<br>17.745 | -0.55%<br>19.894<br>19.786 | -0.61%<br>22.007<br>21.875 | -0.56%<br>23.064<br>22.936 | -0.49%<br>24.121<br>24.004 | -0.41%<br>25.177<br>25.075 | -0.26%<br>26.234<br>26.166 | +0.07%<br>28.348<br>28.366 | +0.48%<br>30.461<br>30.607 |
| 1 | | | | +0.05%<br>17.504<br>17.512 | -0.29%<br>19.684<br>19.627 | -0.42%<br>21.864<br>21.772 | -0.34%<br>22.954<br>22.877 | -0.29%<br>24.044<br>23.975 | -0.23%<br>25.134<br>25.076 | -0.15%<br>26.224<br>26.184 | +0.04%<br>28.404<br>28.415 | +0.32%<br>30.584<br>30.682 |
| 2.5 | | | | -0.07%<br>17.044<br>17.031 | +0.06%<br>19.335<br>19.346 | -0.06%<br>21.626<br>21.612 | -0.03%<br>22.771<br>22.765 | +0.04%<br>23.917<br>23.925 | +0.04%<br>25.062<br>25.071 | +0.001%<br>26.208<br>26.208 | -0.04%<br>28.499<br>28.486 | -0.04%<br>30.790<br>30.776 |
| 5 | | | | | +0.39%<br>18.775<br>18.848 | +0.72%<br>21.20<br>21.353 | +0.94%<br>22.413<br>22.625 | +0.97%<br>23.625<br>23.857 | +0.95%<br>24.838<br>25.076 | +0.86%<br>26.050<br>26.275 | +0.52%<br>28.475<br>28.625 | +0.21%<br>30.90<br>30.965 |
| 7.5 | | | | | | +0.73%<br>20.966<br>21.120 | +1.18%<br>22.246<br>22.512 | +1.32%<br>23.526<br>23.841 | +1.27%<br>24.806<br>25.126 | +1.05%<br>26.086<br>26.364 | +0.51%<br>28.646<br>28.792 | -0.08%<br>31.206<br>31.181 |
| 10 | | | | | | +0.12%<br>20.918<br>20.943 | +0.78%<br>22.266<br>22.440 | +1.06%<br>23.613<br>23.867 | +0.95%<br>24.961<br>25.199 | +0.67%<br>26.308<br>26.485 | -0.18%<br>29.003<br>28.950 | -0.93%<br>31.698<br>31.406 |
| 15 | | | | | | | +0.52%<br>22.613<br>22.732 | +0.80%<br>23.976<br>24.168 | +0.75%<br>25.338<br>25.530 | +0.52%<br>26.701<br>26.839 | -0.15%<br>29.426<br>29.382 | -0.66%<br>32.151<br>31.940 |
| 20 | | | | | | | | +4.7%<br>24.336<br>25.536 | +2.3%<br>25.713<br>26.329 | +1.43%<br>27.091<br>27.483 | +0.38%<br>29.846<br>29.958 | -0.002%<br>32.601<br>32.60 |

(Temperature, [°C] across top; LIQUID PHASE region indicated across lower-left empty cells.)

Note: Underlined numbers represent true value of the dynamic viscosity $\eta_g$

Recommended range of use: (0.1-15)MPa and $(T_{SAT}-530)°C$, with overall accuracy better than 1.33 percent.

This simple correlation ensures good approximation to the dynamic viscosity $\mu_g$ over wide range of pressure and temperature variations of the vapour phase. Accuracy of the approximation is shown in Table 10. In the table the underlined figures represent true values of $\mu_g$, re-calculated from the Reference 1 and shown here also in the upper-right half of Table 8. Above each underlined number there is a number representing the approximation value $\hat{\mu}_g$ and above it the accuracy of

approximation $\epsilon = \dfrac{\mu_g - \hat{\mu}_g}{\mu_g}$, in percent.

Note that the accuracy deteriorates only at very high pressures, about 20 MPa and close to the saturation temperature. Even there it is not worse than 4.7 percent. With increasing temperature and steady pressure the estimate $\hat{\mu}_g$ becomes gradually more precise.

## 4.0 CONCLUSIONS

The demonstrated algorithms provide means for fast and reasonably accurate calculations of variety of heavy water thermodynamic properties. The ranges are suitable for typical CANDU-PHW reactor safety-related studies. Straightforward, compact form of the approximation formulas contribute to simplicity of the programming effort during implementation. In fact, the approximation algorithms are so simple that they have been programmed on the hand-held calculator Hewlett-Packard HP41-C.

The approximation accuracy is good, usually better than 1.3 percent over the wide range of pressure and temperature variations. Only in case of the liquid phase viscosity $\mu_f$ the accuracy deteriorates to about 5 percent. However, even this accuracy is satisfactory when used in calculation of the Reynolds and Prandtl numbers during evaluation of the convective heat transfer coefficients. In commonly used correlations for circular tubes such as Dittus-Boelter or Sieder-Tate equation, the Reynolds number is used with 0.8 exponent and the Prandtl number is used with 0.4 exponent and therefore the effect of approximation inaccuracy is reduced. Nonetheless, a much better accuracy for the $\hat{\mu}_f$ formula can be obtained by correlating the correction coefficient $\beta$ with both temperature and pressure but the resulting algorithm becomes more complicated.

## 5.0   REFERENCES

1.   P.G Hill, R.D. MacMillan, V. Lee, "Tables of Thermodynamic
     Properties of Heavy Water in SI Units", AECL Eng Co 7531,
     Sheridan Park, Mississauga, December 1981.

2.   M. Kacimi, W. Paskievici, "Approximation des Fonctions d'Etat de
     l'Eau Légère et de l'Eau Lourde Dans les États Liquide, Saturé
     et Vapeur Par des Fonctions Linéaires ou Linéarisables Dans le
     Domaine de 1000 à 12000 kPa"; Proceedings of the 4th Annual
     Conference of the Canadian Nuclear Society, Montreal, June 1983.

3.   M. Abramowitz, I.A. Stegun, "Handbook of Mathematical
     Functions", Dover Publications, Inc, New York, December 1972.

4.   L.S. Tong, J. Weisman, "Thermal Analysis of Pressurized Water
     Reactors" - second edition, The American Nuclear Society, La
     Grange Park, Illinois, 1979.

5.   J. Raznjvic, "Handbook of Thermodynamic Tables and Charts",
     McGraw Hill, 1976.